



Optimization of Matching Phase Between Two Driving Oscillations of a TFG Using Diamond-Shaped Frame

Vu Van The^{1(✉)}, Tran Quang Dung¹, and Chu Duc Trinh²

¹ Le Quy Don Technical University, Hanoi, Vietnam
thevutb@gmail.com

² Vietnam National University, Hanoi, Vietnam

Abstract. This paper presents a study on the optimization of matching phase between two outer frames of a MEMS tuning fork gyroscope by using a diamond-shaped frame. The differential motion equations of the system are established and solved via the second Newton law. The obtained results show that the anti-phase mode in driving direction is guaranteed when the exciting forces are applied to two outer frames. Remarkably, when the spring coefficient of the diamond-shaped frame increases 150%, the matching phase between two outer frames raises up 95%.

Keywords: Matching phase · Tuning fork gyroscope · Anti-phase

1 Introduction

MEMS (Micro-Electro-Mechanical System) Vibratory Gyroscope (MVG) is a kind of sensors that is common to measure angular velocity or rotational angle of a subject [1]. Basing on Coriolis principle, the energy transfers from primary vibration to secondary one to support the operation of this sensor [1–3]. The MVGs have many advantages over traditional gyroscopes for their small size, low power consumption, low cost, batch fabrication and high performance [1–7], so they are widely used in a variety of industries.

The MEMS tuning fork gyroscope (TFG) includes two identical tines that vibrate in opposite direction (anti-phase mode) [4–6]. Thanks to this state, the performance of TFG increases significantly. However, an in-phase mode easily appears in the traditional TFG structure with the direct mechanical coupling between two tines [6]. Moreover, any phase deviation of external forces could cause the phase error for two tines of TFG in driving direction, so that the matching phase between two outer frames of TFG decreases considerably. Therefore, it is necessary to design a mechanism to directly connect two tines for the purpose of creating anti-phase mode, where this mechanism plays an important role in optimizing of matching phase between two tines [7].

This paper focuses on demonstrating the ability to increase the matching phase between two outer frames in driving direction of the proposed TFG when they are connected directly by a novel structure called diamond-shaped frame. These outer

frames are expected to vibrate with the absolute anti-phase mode in order to create the anti-phase mode for sensing vibrations of proof-masses in proposed TFG model.

2 Differential Motion Equations of the Proposed TFG

The proposed model TFG consists of two identical tines as shown in Fig. 1. Each tine is defined as a single gyroscope which includes a proof mass m_S and an outer frame m_f . The configuration and dynamic characteristics of every single gyroscope are shown in the reference numbered [8]. They are connected together by a spring-damping system (k_{yi} - c_{yi}) and suspended on substrate thanks to another system (k_{xi} - c_{xi}). Two single gyroscopes are connected together by a diamond-shaped frame to create the proposed TFG. The diamond-shaped frame has four rigid bars with length L and the rectangular cross-section. The bars are connected to the connectors by elastic stems (A, B, C, and D). The diamond-shaped frame is suspended on the substrate by a spring system (k_y).

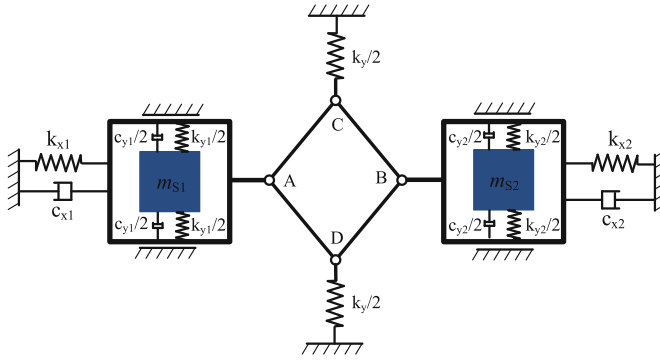


Fig. 1. The configuration of the proposed TFG

The four beams of the diamond-shaped frame are assumed to be absolutely rigid. The displacement at the end of the beams is carried out by the elasticity of stems with the smaller section. The displacement of the point A is x_1 , while the point C displaces y_1 from their initial position. The points B and D are the same displacement with A and C except their direction of motion (see Fig. 2a). These displacements depend on each other and have a relation as follows:

$$y_1 = \sqrt{L^2 - (L_1 - x_1)^2} - L_2; \quad y_2 = \sqrt{L^2 - (L_1 - x_2)^2} - L_2 \quad (1)$$

where $L_1 = L \cos \alpha_0$; $L_2 = L \sin \alpha_0$; α_0 is the angle to define initial position of rigid bars of the diamond-shaped frame.

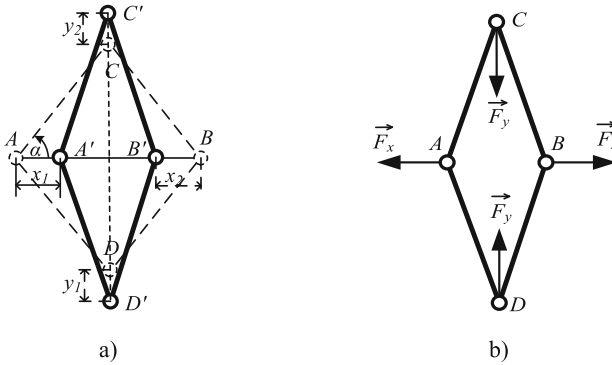


Fig. 2. Schema of deformation (a) and elastic forces (b) of diamond-shaped frame

The elastic force applied to the outer frames in the x -direction is determined as the followed expression:

$$F_x = \frac{1}{2}(F_{Cy} + F_{Dy})\cot\alpha \tag{2}$$

with, α is an angular rotation of a rigid bar at the determined moment.

In this issue, both outer frame and proof mass vibrate in driving direction, so that they are considered as one element with total mass m_1 and m_2 (where $m_i = m_{fi} + m_{Si}$) in order to simplify for the description. The component forces applied to the masses m_1 and m_2 are shown in Fig. 3 after splitting them.

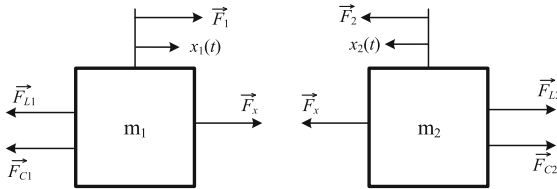


Fig. 3. The schema of forces applied to two outer frames

Where, \vec{F}_1, \vec{F}_2 are external forces applied to the outer frames; $\vec{F}_{L1}, \vec{F}_{L2}$ are elastic forces of the beams with the stiffness coefficients k_{x1}, k_{x2} respectively; $\vec{F}_{C1}, \vec{F}_{C2}$ are damping forces with damping coefficients c_{x1}, c_{x2} known as the slide air damping between the masses and the substrate, \vec{F}_x is elastic force mentioned above.

$$F_{L1} = k_{x1}x_1; F_{L2} = k_{x2}x_2; F_{C1} = c_{x1}\dot{x}_1; F_{C2} = c_{x2}\dot{x}_2 \tag{3}$$

The differential equations of motion for the system are obtained by using the second Newton law and adding some equations describing the geometric relations between the displacements x_1 , x_2 , and y_1 , y_2 , as follows:

$$\begin{cases} m_1\ddot{x}_1 + c_{x1}\dot{x}_1 + k_{x1}x_1 + \frac{k_y}{4} \left(\sqrt{L^2 - (L_1 - x_1)^2} + \sqrt{L^2 - (L_1 - x_2)^2} - 2L_2 \right) \cot\alpha = F_1 \\ m_2\ddot{x}_2 + c_{x2}\dot{x}_2 + k_{x2}x_2 + \frac{k_y}{4} \left(\sqrt{L^2 - (L_1 - x_1)^2} + \sqrt{L^2 - (L_1 - x_2)^2} - 2L_2 \right) \cot\alpha = F_2 \\ \alpha = \text{atan} \left(\left(\sqrt{L^2 - (L_1 - x_1)^2} - L_2 \right) / x_1 \right) \\ L_1 = L \cos \alpha_0; L_2 = L \sin \alpha_0 \end{cases} \tag{4}$$

3 Matching Phase in Driving Direction

The characteristic parameters of the proposed TFG are shown in Table 1.

Table 1. The parameters of TFG

Parameter	Value	Unit
Mass of the left single gyroscope: m_1	2.65×10^{-7}	kg
Mass of the right single gyroscope: m_2	2.65×10^{-7}	kg
Driving stiffness of the left single gyroscope: k_{x1}	25.2	N/m
Driving stiffness of the right single gyroscope: k_{x2}	25.2	N/m
Damping coefficient in left drive direction: c_{x1}	2×10^{-5}	kg/s
Damping coefficient in right drive direction: c_{x2}	2×10^{-5}	kg/s
Length of a rigid bar: L	10^{-4}	m
Initial angle of rigid bar: α_0	60°	degree

3.1 Amplitude-Frequency Response

The external harmonic force applied to outer frames has a form as follows:

$$F_1 = F_0 \sin(2\pi ft + \alpha_1); F_2 = F_0 \sin(2\pi ft + \pi + \alpha_2) \tag{5}$$

Expressions (5) are defined by the force value F_0 and the exciting frequency f . The phase deviation of two external forces is defined by the followed expression:

$$\alpha_d = \alpha_1 - \alpha_2 \tag{6}$$

where α_1 and α_2 is the phase angle of external force F_1 and F_2 respectively. The phase deviation which is called the external phase deviation is $\alpha_d = 0$ to guarantee the absolutely opposite direction of two external forces.

The parameters f and F_0 are determined by surveying amplitude - frequency response for the system. In order to reduce the time of the calculation and guarantee the efficiency, the exciting frequency of the system is considered from 1400 to 1800 Hz. According to the results shown in Fig. 4, the exciting frequency should be 1590 Hz.

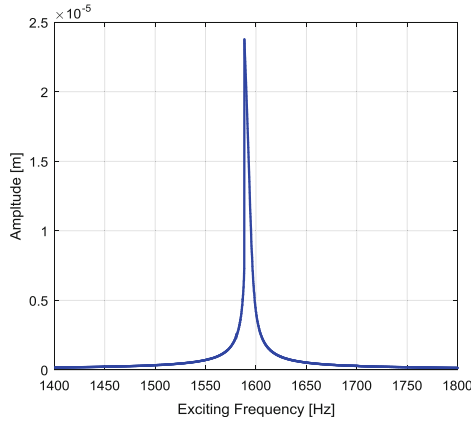


Fig. 4. Amplitude-frequency response

When the external force with the above expression (5) applied to two outer frames, their stable vibrations in driving direction are harmonic functions as shown in Fig. 5. Due to the absolute opposite direction of two exciting force, the anti-phase mode of these vibrations is assured completely.

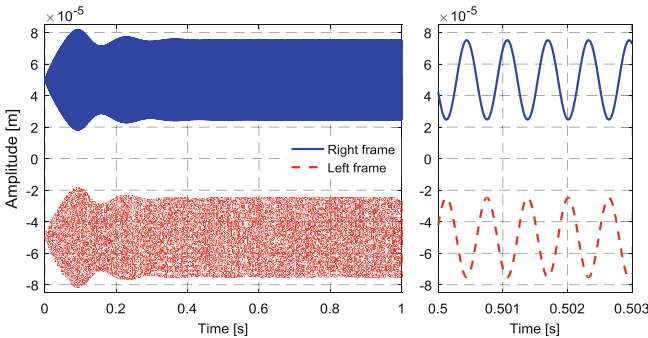


Fig. 5. Driving mode with external harmonic forces

3.2 Matching Phase Between Two Outer Frames

The external forces applied to the outer frames are defined as electrostatic forces with opposite phases (anti-phase). However, in fact, the error may appear in the phase between two external forces ($\alpha_d \neq 0$), hence, the mechanical phase deviation in the responses of the outer frames will appear.

When k_x is changed with some specific values, the effect of spring coefficient k_y on the matching phase between two outer frames is shown in Fig. 6. According to this result, when the stiffness of the beam in the y -direction increases, the system could adjust to decreasing the mechanical phase deviation of two outer frames in driving direction. Especially, when k_y increase from 10 N/m to 25 N/m, with the external phase deviation (20°), the matching phase increases from 91.25% ($1.75^\circ/20^\circ$) to 95% ($1^\circ/20^\circ$) respectively (see Table 2). So, the diamond-shaped frame could optimize of matching phase between the outer frames.

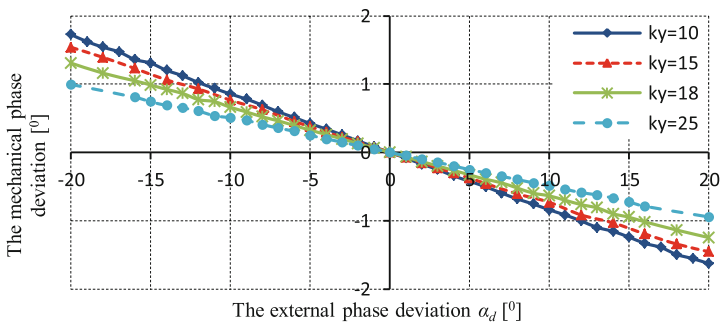


Fig. 6. Phase deviation in driving direction between two outer frames

Table 2. Optimizing of matching phase in driving mode

Spring coefficient of frame k_y (N/m)	10	15	18	25
Phase deviation of driving mode ($^\circ$)	1.75	1.5	0.065	0.05
Matching phase in driving mode	91.25%	92.5%	93.5%	95%

4 Conclusion

The paper introduces a TFG model with connecting frame named diamond-shaped frame for the purpose of directly linking two single gyroscopes in two sides of this frame to create a TFG with an anti-phase mode in driving direction. The differential equations of two outer frames are set up to describe the displacements of TFG outer frames and their relation. The vibrations of outer frames are studied to demonstrate that the driving vibrations of the outer frames have completely opposite phase thanks to the

diamond-shaped frame. The results show that the matching phase is improved from 91.25% to 95% in comparison with without diamond-shaped frame. It is a base to study the sensing mode in the proposed TFG for the purpose of increasing the performance of the sensor.

References

1. Acar, C., Shkel, A.M.: MEMS Vibratory Gyroscopes - Structural Approaches to Improve Robustness. Springer (2009)
2. Shkel, A.M.: Dynamics and control of micromachined gyroscopes. In: Proceedings of the American Control Conference, pp. 2119–2124, June 1999
3. Sang, H., Wen, Y.: Modeling and simulation for a vibratory tuning-fork MEMS gyroscope. In: Third International Conference on Measuring Technology and Mechatronics Automation, pp. 605–608, June 2011
4. Apostolyuk, V., Tay, F.E.H.: Dynamics of micromechanical coriolis vibratory gyroscopes. *Sens. Lett.* **2**(4), 1–8 (2005)
5. Choi, B.: Dynamic characteristics of vertically coupled structures and the design of a decouple micro-gyroscope **8**, 3706–3718 (2008). www.mdpi.org/sensors
6. Guan, Y.W., Gao, S.Q., Jin, L., Cao, L.M.: Design and vibration sensitivity of a Mems tuning fork gyroscope with anchored coupling mechanism. *Microsyst. Technol.* **22**, 247–254 (2016)
7. Guan, Y.W., Gao, S.Q., Liu, H., Lei, J., Niu, S.: Design and vibration sensitivity analysis of a MEMS tuning fork gyroscope with an anchored diamond coupling mechanism. *Sensors* **16**, 468–483 (2016)
8. Vu, V.T., Dung, T.Q., Trinh, C.D.: Dynamic analysis of a single MEMS vibratory gyroscope with decoupling connection between driving frame and sensing proof mass. *Int. J. Appl. Eng. Res.* **13**(17), 5554–5561 (2017)